Published in final edited form as:

Biochemistry. 2010 November 09; 49(44): 9584–9593. doi:10.1021/bi101391z.

Effects of Oxidation on Structural Stability and Remodeling of Human Very Low Density Lipoprotein†

Madhumita Guha and **Olga Gursky***

Department of Physiology and Biophysics, Boston University School of Medicine, Boston, Massachusetts 02118, United States

Abstract

Very low density lipoproteins (VLDL) are triglyceride-rich precursors of low-density lipoproteins (LDL) and a risk factor for atherosclerosis. The effects of oxidation on VLDL metabolism may be pro- or antiatherogenic. To understand the underlying biophysical basis, we determined the effects of copper (that preferentially oxidizes lipids) and hypochlorite (that preferentially oxidizes proteins) on the heat-induced VLDL remodeling. This remodeling involves VLDL fusion, rupture, and fission of apoE-containing high-density lipoprotein- (HDL-) like particles; HDL with similar size, density, and protein composition are formed upon VLDL remodeling by lipoprotein lipase, a key enzyme in triglyceride metabolism. Circular dichroism, turbidity, and electron microscopy show that mild oxidation promotes VLDL fusion and rupture, while advanced oxidation hampers these reactions. VLDL destabilization upon moderate oxidation results, in part, from the exchangeable apolipoprotein modifications, including proteolysis and limited cross-linking. VLDL stabilization against fusion and rupture upon advanced oxidation probably results from massive protein cross-linking on the particle surface. Electron microscopy and gel electrophoresis reveal that oxidation promotes fission of apoE-containing HDL-size particles; hydrolysis of apolar core lipids probably contributes to this effect. Copper and hypochlorite have similar effects on VLDL remodeling, suggesting that these effects may be produced by other oxidants. In summary, moderate oxidation that encompasses *in vivo* conditions destabilizes VLDL and promotes fission of HDL-size particles. Consequently, mild oxidation may be synergistic with lipoprotein lipase reaction and, hence, may help to accelerate VLDL metabolism.

Very low density lipoproteins (VLDL)[1] transport triacylglycerides (TG) and cholesterol, mainly in the form of cholesterol esters (CE), from the liver to the peripheral tissues. Elevated plasma levels of TG are a hallmark of metabolic syndrome (1–4) that is associated

†This work was supported by National Institutes of Health Grants GM067260 and HL026355.

*Corresponding author. Tel: (617) 638-7894. Fax: (617) 638-4207. gursky@bu.edu.

SUPPORTING INFORMATION AVAILABLE

Figures showing (S1) circular dichroism spectra of intact and copper-oxidized VLDL, (S2) effects of copper oxidation on thermal stability of VLDL, (S3) effects of oxidation on VLDL morphology at ambient temperatures, and (S4) oxidative changes in the exchangeable apolipoproteins in VLDL assessed by SDS–PAGE and immunoblotting. This material is available free of charge via the Internet at http://pubs.acs.org.

[1]Abbreviations: VLDL, very low density lipoprotein; IDL, intermediate-density lipoprotein; LDL, low-density lipoprotein; HDL, high-density lipoprotein; LpL, lipoprotein lipase; apo, apolipoprotein; TG, triacylglycerol; MG, monoacylglycerol; CE, cholesterol ester; PE, phosphatidylethanolamine; PC, phosphatidylcholine; FFA, free fatty acids; CD, circular dichroism; T-jump, temperature jump; EM, electron microscopy; SDS, sodium dodecyl sulfate; PAGE, polyacrylamide gel electrophoresis.

with increased risk of cardiovascular disease, stroke, and type 2 diabetes (5, 6). VLDL is also a metabolic precursor of low-density lipoprotein (LDL, or “bad cholesterol”) and an independent risk factor for atherosclerosis (7–10). VLDL clearance and maturation to LDL involve extensive remodeling by plasma factors (Figure 1) (2, 11). Plasma levels of VLDL are determined by the balance among the rates of VLDL synthesis, remodeling, and clearance, which are targets of lipid-lowering therapies such as statins, fibrates, and omega-3 fatty acids (12–14).

VLDL are synthesized by the liver as heterogeneous particles (d = 30–100 nm) containing a core of apolar lipids (mainly TG and CE) and an amphipathic surface comprised of polar lipids (mainly phosphatidylcholines, PCs) and proteins (termed apolipoproteins). Apolipoproteins cover a large fraction of the particle surface, from about 20% in VLDL up to 80% in HDL (15), and are essential for lipoprotein stabilization and remodeling via the interactions with plasma enzymes, cofactors, lipid transporters, and cell receptors. The VLDL proteins include one copy of the nonexchangeable (water-insoluble) apoB (9) and multiple copies of the exchangeable proteins, apoE and apoCs (Figure 1). The rate-limiting step in VLDL remodeling is hydrolysis of core TG by lipoprotein lipase (LpL) (16–20). LpL reaction generates excess surface material that dissociates from VLDL in the form of small dense high-density lipoproteins (HDL) that contain only exchangeable proteins, apoE and apoCs (21, 22) (Figure 1). Such apoE-containing particles comprise about 10% of plasma HDL and play important roles in lipid metabolism (22). The VLDL remnants generated by LpL are cleared by the cell receptors or further remodeled to form LDL (2, 11).

Modifications such as oxidation and glycation, which have been demonstrated to occur *in vivo* during the lifetime of apoB-containing lipoproteins (hours to days) (ref 23 and references therein), affect VLDL remodeling and clearance via multiple pathways that are not fully understood. The effects of VLDL oxidation on atherogenesis are also not entirely clear (24). Multiple lines of evidence suggest that, similar to LDL, oxidation of VLDL triggers a cascade of proatherogenic and proinflammatory responses, including lipoprotein retention in the arterial wall, enhanced VLDL uptake by arterial macrophages, macrophage CE accumulation, foam cell formation, and deposition of atherosclerotic plaques (25–31). *In vivo* lipoprotein oxidation is thought to occur mainly via the action of prooxidant enzymes in the arterial wall. *In vitro* lipoprotein oxidation by various agents induces a wide array of modifications in lipids (e.g., peroxidation of unsaturated fatty acids in phospholipids, cholesterol, and TG, followed by formation of aldehydes and ketones that modify Lys groups, etc.) and proteins (modifications of aromatic and Lys groups, proteolysis, cross-linking, etc.). The pro- or antiatherogenic effects of these modifications and their relevance to *in vivo* conditions have been intensely investigated, yet the exact form(s) in which oxidized lipoproteins exist *in vivo* and their pathological significance are not well-defined (24, 32, 33). The consensus is that the most physiologically relevant species is the “minimally oxidized” lipoprotein that carries lipid peroxides and their products but has minimal protein modifications.

Furthermore, there is an emerging consensus that lipoprotein oxidation is not always proatherogenic (24). It was first prompted by the failure of antioxidants to alleviate the risk of cardiovascular disease in clinical trials (refs 3, 24, 32, and 33 and references therein).

Further support comes from the prooxidant effects of TG-lowering therapies such as fibrates or omega-3 fatty acid; moreover, healthy cardioprotective activities such as aerobic exercise and moderate consumption of alcohol are also prooxidant (refs 14, 24, and 34 and references therein). This suggests that oxidation is not always detrimental for lipoprotein metabolism and cardioprotection.

Our goal is to provide the biophysical basis for understanding the effects of oxidation on VLDL remodeling. To this end, we use thermal denaturation as a model for the analysis of the effects of oxidation on such remodeling. Earlier we showed that, similar to HDL and LDL, thermal disruption of native VLDL is a slow kinetically controlled transition that involves lipoprotein fusion and rupture (35–37). In contrast to other lipoproteins, VLDL heating also leads to fission of HDL-size particles. Biochemical analysis of these small dense particles (10–12 nm, 1.11–1.19 g/mL) showed that they contain CE and TG in their core and PCs and exchangeable proteins, apoE and probably apoCs, in their surface (37). These particles closely resemble a subclass of plasma HDL generated during VLDL remodeling by LpL (Figure 1) (20, 21, 37). Fission of these HDL-like particles upon VLDL heating is accompanied by fusion of the remnant lipoproteins followed by lipoprotein rupture and release of apolar core lipids that coalesce into large droplets (37) whose size and morphology are similar to the lipid droplets found in atherosclerotic plaques (38). Thus, thermal denaturation mimics key aspects of VLDL remodeling *in vivo* and provides a useful model to study this remodeling. We use this model to test the effects of oxidation on VLDL remodeling.

Compared to extensive analyses of LDL and HDL oxidation, relatively few studies have addressed VLDL oxidation *in vitro*. These studies have been mainly focused on advanced oxidation (26–28, 39), particularly by Cu^{2+}, a radical oxidant that preferentially oxidizes lipids (26, 27, 39–41). No studies of the effects of oxidation on VLDL remodeling have been reported. Because of the experimental difficulties in biophysical characterization of the large heterogeneous lipid-loaded particles, stability studies have been limited to nonmodified VLDL (37).

Here we report the first analysis of the effects of oxidation on structural stability and remodeling of VLDL. In addition to copper, we use hypochlorite, an oxidant that preferentially reacts with proteins (42) and is a product of myeloperoxidase, one of the enzymes that oxidize lipoproteins in the arterial wall and at the sites of inflammation (28, 42). We analyze structural stability of VLDL that were modified by Cu^{2+} or OCl^{-} to various degrees. The results reveal that oxidation has distinct effects on VLDL remodeling, which show similar trends for different oxidants and depend critically on the oxidation degree: Interestingly, mild oxidation that probably approximates minimal lipoprotein oxidation *in vivo* (33) destabilizes VLDL and promotes fission of the excess surface material in the form of apoE-containing HDL-size particles. This suggests that mild oxidation may be synergistic with the LpL reaction.

MATERIALS AND METHODS

VLDL Isolation and Sample Preparation

Plasma VLDL from nine healthy volunteer donors were used. Plasma was donated at a local blood bank in full compliance with the regulations of the Institutional Review Board. Single-donor VLDL were isolated from EDTA-treated plasma by density gradient ultracentrifugation in the density range 0.94–1.006 g/mL (43). Total VLDL migrated as a single band on agarose gel (Figure 2, lane 0). Human VLDL are comprised of two main subclasses, $VLDL_1$ (d = 60–100 nm) and $VLDL_2$ (d = 35–60 nm), containing one molecule of apoB per particle and various amounts of apoE and apoCs which are greater in larger particles. To improve sample homogeneity, $VLDL_2$ was separated from the total VLDL by an additional round of ultracentrifugation at 40000 rpm for 30 min at 4 °C (37) and was used to record the data from the OCl-treated particles shown in this paper. Spectroscopic data of $VLDL_2$ and of total plasma VLDL (that was used to record the copper oxidation data shown in this paper, as well as some hypochlorite data) were similar. Donor- and diet-specific variations in lipoprotein composition resulted in small batch-to-batch variations in VLDL stability; hence, the exact oxidation stages at which the maximal VLDL destabilization and fission of small particles were observed, as well as the particle size distribution and the amounts of the small particles, varied from batch to batch. However, the general trends observed upon VLDL oxidation were similar for all batches explored; hence, lipoprotein heterogeneity did not affect the key conclusions of this study.

VLDL stock solution of 0.4–2.5 mg/mL protein concentration was dialyzed against 10 mM sodium phosphate, 0.25 mM EDTA, and 0.02% NaN_3, pH 7.6, which was a standard buffer used throughout this work. For copper oxidation, EDTA was removed by dialysis against EDTA-free standard buffer (10 mM sodium phosphate, 0.02% NaN_3, pH 7.6). The VLDL stock solution was stored in the dark at 4 °C and was used over 4 weeks during which no protein degradation was detected by SDS–PAGE and no changes in the protein secondary structure or lipoprotein stability were observed by CD spectroscopy and turbidity.

VLDL Oxidation and Biochemical Characterization

For copper oxidation, VLDL solution of 0.2–0.5 mg/mL protein concentration in EDTA-free standard buffer was equilibrated at 37°C, followed by the addition of $CuSO_4$ to the final concentration of 5 μM. To obtain VLDL oxidized to various stages, the reaction was stopped after 1–48 h (marked 1–6 in Figure 2A,B) by addition of 1 mM EDTA, followed by sample cooling on ice. VLDL incubation with $CuSO_4$ for over 5 days produced turbid samples that were not used for further studies. To obtain VLDL oxidized by OCl^- to various stages, we modified the well-established protocols that were used in oxidation studies of HDL and LDL (refs 44 and 45 and references therein). VLDL solution of 0.5 mg/mL protein concentration in standard buffer was incubated at 37°C for 5 h with NaOCl solutions of 0.02–10 mM concentrations (marked 1–6 in Figure 2C), followed by extensive dialysis against the standard buffer. Concentration of freshly prepared NaOCl was determined spectrophotometrically using a molar absorption coefficient of 350 cm^{-1} at 292 nm. The concentrations of OCl^-, which varied from batch to batch depending on the VLDL stability (higher for more stable VLDL that required higher amounts of oxidant to attain similar

changes in stability), ranged from 0.02 to 0.09, 0.1 to 0.2, 0.3 to 0.6, 0.7 to 0.9, 1.0 to 2.0, and 5.0 to 10.0 mM to produce VLDL at oxidation stages 1 to 6, respectively. Similarly, the incubation times with Cu^{2+} varied from batch to batch and were higher for more stable particles.

A Varian Cary 300 UV/visible absorption spectrometer equipped with a thermoelectric temperature control was used to monitor the time course of copper-induced lipid peroxidation by measuring UV absorbance at 234 nm for conjugated diene formation (40). The spectrometer was also used to record near-UV/vis absorption spectra (350–600 nm) at 25 °C of VLDL oxidized to various stages by Cu^{2+} or OCl^{-} to monitor consumption of carotenoids (ref 44 and references therein).

Agarose-based Titan gel lipoprotein electrophoresis was used to monitor changes in VLDL charge upon oxidation. Such changes occur due to oxidative modifications of Lys and formation of free fatty acids upon PC lipolysis, leading to increased net negative charge on VLDL (ref 47 and references therein). Thin-layer chromatography was used to monitor changes in lipid composition upon VLDL oxidation.

To monitor apolipoprotein fragmentation and cross-linking that is induced by oxidation, sodium dodecyl sulfate (SDS)–polyacrylamide gel electrophoresis (PAGE) was performed using a 4%, 12%, or 20% homogeneous system for apoB (550 kDa), apoE (32 kDa), or apoC-III (8.8 kDa), respectively. The gels were run at 120 V for 20, 60, or 120 min, respectively, followed by staining with Imperial protein stain. Alternatively, the gels were transferred to polyvinylidene fluoride membranes at 100 V for 1 h, and the membranes were probed with primary monoclonal antibody to apoB (1D1 from Lipoprotein and Atherosclerosis Research Group, University of Ottawa Heart Institute) or with polyclonal antibodies to apoE (Chemicon) or apoC-III (Chemicon Internationals). Secondary antibodies for polyclonal goat were from Biodesign, and rabbit antibodies were custom made by Sigma. The blots were probed with horseradish peroxidase-conjugated secondary antibodies (Sigma) and visualized using an enhanced chemiluminescent system (Perkin-Elmer).

To assess changes in the particle size upon oxidation to various stages, nondenaturing gradient gel electrophoresis was carried out by using a 4–20% gradient run on a large-format BRL system for 4 h. The gels were stained with Imperial protein stain. Particle diameters were assessed from comparison with the protein markers (Amersham Biosciences). For immunoblotting, the samples were subjected to nondenaturing gradient gel electrophoresis, transferred to polyvinylidene fluoride membrane for 24 h, and probed with primary antibodies to apoE or apoB. VLDL at various stages of oxidation were visualized at 25 °C by negative staining EM using a CM12 transmission electron microscope (Philips Electron Optics) as described (35).

Circular Dichroism (CD) Spectroscopy and Turbidity

To assess lipoprotein structure and stability, CD and turbidity data were recorded using AVIV-400 or AVIV-62DS spectrometers with thermoelectric temperature control (35, 37). VLDL solutions of 0.1 mg/mL protein concentrations were placed in 1 mm path length cells to record far-UV CD spectra (190–250 nm) to monitor protein secondary structure. Far-UV

CD data were normalized to protein concentration and expressed as molar residue ellipticity, [Θ]. VLDL solutions of 0.5 mg/mL protein were placed in 2 mm path length cells to record near-UV/vis CD (250–500 nm). Although near-UV CD is usually used to report on aromatic packing in the tertiary protein structure, it does not provide a sensitive tool for monitoring changes in aromatic packing in apoB on the lipoprotein surface. Moreover, in ruptured LDL and VLDL, near-UV/vis CD spectra are strongly dominated by induced CD of lipids. A large negative CD peak centered at 320 nm in these spectra reported on lipid repacking upon particle rupture and release of apolar core lipids that coalesce into large droplets (37, 45). Thus, we used near-UV CD to monitor VLDL rupture and coalescence into lipid droplets. To monitor VLDL rupture as a function of temperature, CD melting data, $\Theta_{320}(T)$, were recorded at 320 nm during sample heating and consecutive cooling from 25 to 98 °C at a constant rate of 11 °C/h. Heat-induced increase in the particle size due to VLDL fusion followed by rupture and coalescence into large lipid droplets was monitored by measuring dynode voltage V, which is proportional to turbidity in CD experiments (47). Turbidity and CD melting data, $V_{320}(T)$ and $\Theta_{320}(T)$, were measured simultaneously at 320 nm. The apparent transition temperatures T_m were determined from the peak positions in the first derivative of the melting data, $dV_{320}(T)/dT$ (for fusion and rupture) and $d\Theta_{320}(T)/dT$ (for rupture). In the kinetic temperature jump (T-jump) experiments, the sample temperature was rapidly increased at $t = 0$ from 25 °C to a higher constant value (75–98 °C), and the time course of VLDL fusion and rupture was monitored at 220 nm by turbidity, $V_{320}(t)$, as described (37).

RESULTS

Effects of Oxidation on the Secondary Structure of VLDL Proteins

VLDL were oxidized by copper or hypochlorite to various stages (marked 1–6 in Figure 2). To characterize the protein secondary structure, far-UV CD spectra were recorded from VLDL that were modified by OCl^- (Figure 3A) or Cu^{2+} (Supporting Information Figure S1). Intact VLDL showed a mixture of α-helix and β-sheet that varied with the particle size. The spectra of $VLDL_2$ (smaller particles whose major protein, apoB, has high β-sheet content) showed predominantly β-sheet conformation, while those of total VLDL (a mixture of $VLDL_2$ and larger $VLDL_1$ particles that have greater amounts of highly helical proteins, apoE and apoCs) indicated higher α-helical content (black lines in Figure 3A and Supporting Information Figure S1). VLDL oxidation by OCl^- or Cu^{2+} led to a gradual loss of this secondary structure (Figure 3A and Supporting Information Figure S1). Similarly, partial loss of secondary structure in apoB was observed upon LDL oxidation (45, 48). $VLDL_2$ showed substantial β-sheet unfolding in apoB, as illustrated by the difference spectrum between the intact particles and those oxidized to stage 6. This difference spectrum showed a negative CD peak centered near 218 nm, which is characteristic of the β-sheet (Figure 3A, insert). A similar difference spectrum of total VLDL that contain larger fraction of α-helical proteins showed two negative CD peaks centered at 208 and 222 nm, indicating partial helical unfolding in these proteins (Supporting Information Figure S1A). In addition to protein secondary structure, far-UV CD of VLDL and LDL can be significantly affected by the induced CD from lipids, specifically, a large negative peak centered near 320 nm that dominates the CD spectra of ruptured lipoproteins (36, 37). The absence of such a peak in

the spectra of oxidized VLDL at ambient temperatures (Figure 3B and Supporting Information Figure S1B), together with the corresponding EM data (Figure 6 and Supporting Information Figure S3), showed that the lipoproteins used in these experiments did not rupture upon oxidation at 37 °C. Consequently, far-UV CD changes observed upon VLDL oxidation resulted entirely from the changes in the protein secondary structure. In summary, oxidation by OCl^- or Cu^{2+} leads to progressive unfolding of some of the secondary structure in VLDL proteins, including β-sheets in apoB and α-helices in apoE and apoCs.

Effects on VLDL Stability and Morphologic Transitions

To test whether partial unfolding of the secondary structure upon oxidation destabilizes the lipoprotein assembly, VLDL were oxidized to various stages by OCl^- or Cu^{2+}, and their thermal stability was assessed by heating at a rate of 11 °C/h from 25 to 98 °C. CD and turbidity melting data, $\Theta_{320}(T)$ and $V_{320}(T)$, were recorded simultaneously at 320 nm to monitor repacking of apolar core lipids upon lipoprotein rupture (by CD) and increase in the particle size upon lipoprotein fusion and rupture (by turbidity) (36, 37, 47). Figure 4 shows turbidity and CD melting data recorded of OCl-treated VLDL, and Supporting Information Figure S2 shows similar data of Cu-treated VLDL. Initially, progressive oxidation led to large low-temperature shifts in the melting curves (by −18 °C at stage 4, Figure 4A, C), indicating VLDL destabilization. Interestingly, this trend was reversed at later stages, as evident from the high-temperature shifts in the CD and turbidity melting data, indicating increased stability (stages 4–6, Figure 4B,D). These shifts were accompanied by a large reduction in the transition amplitude, suggesting that the particles formed upon heating of extensively oxidized VLDL were smaller than those formed upon similar heating of intact or moderately oxidized VLDL. Melting data of Cu-treated VLDL showed similar trends (Supporting Information Figure S2A,B). Consequently, these trends were not specific to a particular oxidation mechanism and resulted from the products that are common to radical and nonradical oxidants.

Figure 4E shows the apparent transition temperature T_m (determined from the first derivatives of the melting data in Figure 4A–D) as a function of oxidation degree. This plot illustrates that (i) particle fusion precedes rupture and (ii) the temperature of fusion and rupture first decreases and then increases upon oxidation, with minimal T_m (corresponding to lowest VLDL stability) observed near stage 4 of OCl^- oxidation (Figure 4E). Although the exact oxidation stage at which minimal VLDL stability was observed varied from batch to batch, the overall trend was similar for all VLDL batches explored.

The effects of oxidation on the particle stability were further tested in the kinetic experiments. VLDL were oxidized by OCl^- or Cu^{2+} to various stages, the sample temperature was rapidly raised to a higher constant value, and the time course of VLDL fusion and rupture was monitored by turbidity, $V_{220}(t)$ (37). Figure 5 shows selected data recorded in a T-jump to 80 °C of OCl-treated VLDL, and Supporting Information Figure S2C shows similar data of Cu-treated VLDL. These and other kinetic data clearly show that moderate oxidation, which probably encompasses *in vivo* conditions, accelerates heat-induced fusion and rupture and, hence, destabilizes VLDL (Figure 5A and Supporting Information Figure S2C). In contrast, more extensive oxidation (to stage 4 and beyond)

decelerates VLDL disruption and greatly reduces its amplitude, so the transition vanishes upon advanced oxidation (stage 6, Figure 5B). These results are consistent with the melting data in Figure 4. Taken together, our kinetic and melting data of OCl^- or Cu-treated VLDL clearly show that moderate oxidation destabilizes VLDL and accelerates its fusion and rupture, while extensive oxidation hampers these transitions (Figures 4 and 5 and Supporting Information Figure S2).

Negative stain EM was used to visualize VLDL at various stages of oxidation and/or thermal denaturation. Figure 6A–C and Supporting Information Figure S3D show selected electron micrographs of Cu-treated VLDL at various stages of oxidation, and Supporting Information Figure S3A–C shows similar micrographs of OCl-treated VLDL. These and other EM data demonstrate that moderate oxidation to stages 1 and 2 has no detectable effects on VLDL morphology. Interestingly, more extensive oxidation to stages 3–6 leads to progressive VLDL remodeling into heterogeneous larger and smaller particles (Figure 6B,C), along with occasional appearance of large non-spherical particles (Supporting Information Figure S3D). Large particles (>100 nm) are likely products of VLDL fusion, while small particles (~10 nm) are probably produced by fission of the excess surface material from VLDL. Similar large and small particles were observed upon OCl-induced oxidation (Supporting Information Figure S3A,C). To assess the size and protein composition of these small particles, VLDL were oxidized to various stages and analyzed by nondenaturing gradient gel electrophoresis followed by immunoblotting for apoE or apoB (Figure 6D–F). The results revealed that extensive oxidation leads to formation of small particles containing apoE but not apoB (lane 6 in Figure 6D–F). The diameter of these particles estimated from the comparison with molecular size standards ranges from about 8–13 nm (boxed area in Figure 6E), which is in agreement with the EM data (Figure 6C). This diameter is typical of human plasma HDL (d = 8–13 nm).

Earlier we showed that HDL-like particles containing a core of apolar lipids (CE and TG) and a surface of polar lipids (PCs) and exchangeable proteins (apoE and probably apoCs), but not apoB, are formed upon heating of nonoxidized VLDL beyond 80 °C (37). These small particles closely resemble apoE-containing plasma HDL that are generated from VLDL upon TG hydrolysis by LpL (20–22, 37). The results in Figure 6 and Supporting Information Figure S3 show that apoE-containing HDL-size particles can also fission from VLDL upon oxidation. Accurate biochemical analysis of these small particles, which required isolation of a homogeneous density fraction, was hampered by their limited amounts and heterogeneity, which showed batch-to-batch variations and also varied depending on the oxidation stage. However, EM data of all batches explored invariably showed small spheroid particles, rather than stacks of “disks” characteristic of nascent HDL that are devoid of lipid core and stack on edge in negative stain (49). Thus, negative stain EM suggests that the small particles formed upon VLDL oxidation contain apolar core lipids and, hence, resemble mature HDL. Taken together, our results indicate that apoE-containing spheroid HDL-size particles can fission from VLDL not only upon TG hydrolysis or heating but also upon extensive oxidation.

Next, VLDL were visualized by EM at various stages of oxidation before and after heating to 98 °C. The EM data showed that, similar to nonoxidized VLDL (37), mildly oxidized

VLDL undergo heat-induced morphologic transitions that involve lipoprotein fusion, rupture, and fission of HDL-like particles that are similar to those observed upon extensive oxidation (Figure 7B,C). In contrast to intact or mildly oxidized VLDL that undergo heat-induced rupture and coalescence into large lipid droplets making the sample turbid (Figure 7B) (37), extensively oxidized VLDL did not form large droplets (Figure 7C,D), and the sample remained transparent even after overnight incubation at 98 °C. This observation was consistent with the large reduction in the amplitude of the thermal transition monitored by turbidity and near-UV CD in extensively oxidized VLDL (stages 5 and 6 in Figures 4 and 5) and clearly showed that extensive oxidation hampers VLDL rupture. Taken together, our results revealed that (i) moderate oxidation accelerates VLDL fusion and rupture, while more extensive oxidation hampers these transitions (Figures 4 and 5 and Supporting Information Figure S2) and (ii) progressive oxidation promotes fission of small apoE-containing particles (Figure 6 and Supporting Information Figure S3) that are similar but probably not identical to HDL-like particles generated upon VLDL heating (Figure 7B) or TG hydrolysis by LpL (20–22, 37).

Biochemical Changes upon VLDL Oxidation

What is the biochemical basis for the observed changes in structural stability and morphologic transformations of oxidized VLDL? To test for oxidative modifications in VLDL proteins, such as proteolysis and cross-linking, VLDL were oxidized to stages 0–6 and analyzed by SDS–PAGE followed by immunoblotting for apoE or apoC-III (Figure 8). The results showed that, consistent with many other studies summarized in ref 33, progressive oxidation led to proteolysis of the full-size apoB (550 kDa) into fragments (dotted box in Figure 8A) that were cross-linked into large aggregates upon advanced oxidation (solid box in Figure 8A). The size of these aggregates (~1000 kDa) suggested cross-linking of apoB with the exchangeable proteins on the surface of one VLDL particle. Furthermore, oxidation-induced proteolysis followed by cross-linking of apoE was observed in our (Figure 8B) and in the earlier studies (50). At stage 1, a fraction of intact apoE (32 kDa) was cleaved into two fragments, the N-terminal 22 kDa and the C-terminal 10 kDa domain (indicated by * and **); this was followed by protein cross-linking into 50–60 kDa aggregates (stages 3 and 4, solid box in Figure 8B). At later stages (5 and 6), these aggregates were not observed on the 12% gel, suggesting that cross-linking to apoB converted them into much larger aggregates that appeared upon advanced oxidation (stages 4–6, solid box in Figure 8A). At any oxidation stage, a substantial fraction of apoE migrated as a monomer that was not cross-linked to other proteins on the VLDL surface and, hence, could fission in the form of apoE-containing HDL. Furthermore, cross-linking of apoC-III into 50–60 kDa aggregates observed at oxidation stages 2–4, which was followed by the disappearance of these aggregates at later stages, closely resembled the cross-linking pattern of apoE (Figure 8B,C). Taken together, these results suggest that a fraction of apoE and apoCs was cross-linked into 50–60 kDa aggregates at oxidation stages 2–4, followed by additional cross-linking to apoB and formation of much larger aggregates on the particle surface at later stages of oxidation (4–6, Figure 8A). This massive protein cross-linking probably hampers VLDL rupture upon extensive oxidation (stages 5 and 6 in Figures 4B,D and 5B and Supporting Information Figures S2 and S4).

What oxidative modifications in VLDL lipids can influence lipoprotein fission, fusion, and rupture? We used absorption spectroscopy and thin-layer chromatography to characterize VLDL at various stages of oxidation. The levels of carotenoids, which are antioxidants in the lipoprotein core, were monitored by the characteristic triple peak in the absorption spectrum at 420–520 nm (Figure 9, top) (ref 44 and references therein). Progressive VLDL oxidation by Cu^{2+} gradually reduced the amplitude of this peak, while OCl^- produced more abrupt changes at stages 4 and 5, indicating consumption of carotenoids. This antioxidant consumption was accompanied by oxidative modifications to VLDL lipids. The most significant changes detected by TLC upon progressive oxidation included (i) the disappearance of phosphatidylethanolamine (PE), possibly due to oxidation of the amino moiety followed by cross-linking, (ii) formation of lysophosphatidylcholine (lysoPC) and free fatty acids (FFA) that are products of PC hydrolysis, (iii) increase in monoacylglycerides (MG) upon oxidative hydrolysis of TG, and (iv) increase in FFA that are products of PC, CE, and TG hydrolysis (Figure 9, bottom). All these changes in lipid composition are consistent with the earlier studies of lipoprotein oxidation (33). In Cu-treated VLDL these changes were gradual, while in OCl-treated VLDL they were more abrupt and occurred at later stages (Figure 9). This is consistent with direct action of Cu^{2+} on the lipoprotein lipids, as opposed to the protein-mediated action of OCl^- . In summary, oxidative modifications in VLDL lipids observed upon antioxidant consumption include disappearance of PE and generation of lysoPC, FFA, and MG upon hydrolysis of PC and TG. This is expected to importantly affect VLDL remodeling and fusion, since even small amounts of lipids with spontaneous negative curvature, such as PE or unsaturated FFA, can accelerate fusion, while those with spontaneous positive curvature such as lysoPC promote fission of small highly curved particles (45, 46). Furthermore, hydrolysis of apolar lipids such as TG and their conversion into more polar lipids, such as MG and FFA, will promote lipid movement from the apolar core to polar surface, producing excess surface material that is expected to promote fission.

DISCUSSION

Oxidation Modulates Lipoprotein Remodeling in Vitro

This work reveals that oxidation alters the rate and the extent of VLDL remodeling in a manner that depends on the degree of oxidation but not on its specific mechanism. Thus, OCl^- that preferentially oxidizes proteins and Cu^{2+} that preferentially oxidizes lipids produce similar effects on VLDL structure, stability, and morphologic transformations (Figures 3–7 and Supporting Information Figures S1–S4). Therefore, these effects result from lipoprotein modifications that are common to different oxidants (such as lipid peroxidation, protein hydrolysis, cross-linking, etc. (33), Figure 9) and reflect general properties of VLDL. Furthermore, the results of this and earlier studies (44, 45, 51) show that the effects of oxidation on the structural stability and remodeling of human HDL, LDL, and VLDL are distinctly different. In contrast to LDL remodeling and fusion that is inhibited upon progressive oxidation *in vitro* (45), but similar to fusion and rupture of HDL (44), fusion and rupture of VLDL are accelerated at early stages of oxidation but inhibited at more advanced stages (Figures 4 and 5 and Supporting Information Figure S2). Furthermore,

fission of HDL-size particles, which is unique to VLDL (37), is promoted upon progressive oxidation (Figures 6–8 and Supporting Information Figure S3).

Biochemical Basis

Reduced structural stability and accelerated remodeling of VLDL upon mild oxidation by either agent may result, in part, from oxidative modifications to the exchangeable apolipoproteins. Modifications of Met and aromatic residues observed in these proteins at early stages of lipoprotein oxidation increase the polarity of these residues and thereby reduce the hydrophobicity of the apolar lipid-binding faces of the amphipathic α-helices in which these groups are located (refs 44, 51, and 52 and references therein). As a result, protein affinity for lipid is reduced, which facilitates protein dissociation from the lipoprotein surface and fusion of the protein-depleted particles (51, 52). Furthermore, partial fragmentation of apoE into N- and C-terminal domains observed by SDS–PAGE upon mild oxidation in our (Figure 8B) and in the earlier studies (50) probably promotes protein dissociation and lipoprotein fusion, since small exchangeable proteins form less stable complexes with lipids than their larger counterparts (53). In addition, generation of FFA upon oxidative lipolysis of PC, TG, and other lipids (Figure 9) is expected to promote lipoprotein fusion and/or rupture (54).

Interestingly, extensive oxidation inhibits VLDL fusion and rupture but promotes fission of small apoE-containing HDL-size particles. In nonoxidized VLDL, fission of such particles is observed only upon heating to about 80 °C (37), yet in extensively oxidized VLDL small particles are formed at 37 °C (Figures 6 and 7 and Supporting Information Figure S3). The enhanced fission is probably due to the combined effects of oxidative modifications to VLDL proteins and lipids. First, protein cross-linking at the particle surface upon extensive oxidation, which was observed by SDS–PAGE (Figure 8), is expected to inhibit VLDL remodeling and fusion. Nonetheless, fission of HDL-like particles containing only exchangeable apolipoproteins, apoE and apoCs (Figure 8), is facilitated by the fact that, even upon extensive oxidation, a significant fraction of these proteins is not cross-linked to the nonexchangeable apoB (Figure 8B, stages 5 and 6) and, hence, is free to dissociate from the parent lipoprotein. One contributing factor to such fission is oxidative hydrolysis of apolar core lipids, CE and TG, which produces FFA, sterols, and MG (Figure 9). These relatively polar products are expected to move from the particle core to surface, producing excess surface material. A similar mechanism probably provides the driving force for fission of apoE-containing HDL upon TG hydrolysis by LpL. Furthermore, fission of small highly curved particles upon VLDL oxidation is probably aided by formation of lysoPC and depletion of PE (Figure 9). Due to its spontaneous positive curvature, lysoPC prevents fusion and promotes fission of lipid bilayers (55). Moreover, lysoPC in complex with PC can spontaneously form small highly curved protein-free particles (56). Hence, generation of lysoPC upon oxidation is expected to stabilize small HDL-size particles. In contrast, PE has spontaneous negative curvature that reduces free energy of the fusion transition state and thereby promotes bilayer fusion (55, 57). Therefore, progressive depletion of PE together with generation of lysoPC upon extensive oxidation is expected to promote fission of small particles.

In summary, fission of apoE-containing HDL-size particles from VLDL upon progressive oxidation is facilitated by several factors, such as (i) a fraction of monomeric apoE that is not cross-linked to apoB, (ii) hydrolysis of apolar core lipids followed by redistribution of lipolytic products such as FFA and MG from core to surface, generating excess surface material, and (iii) hydrolysis of PE and formation of lysoPC and FFA upon PC hydrolysis. Furthermore, cross-linking of apoB and exchangeable proteins on VLDL surface (Figure 8A) probably inhibits VLDL fusion and rupture upon advanced oxidation.

Potential Implications for Lipoprotein Metabolism

Moderate oxidation by OCl^- probably encompasses oxidative conditions in the arterial wall (refs 24, 33, 41, 42, and 44 and references therein); hence its destabilizing effect on VLDL has potentially important metabolic implications. In many macro-molecular systems, global destabilization tends to increase local structural fluctuations that are often necessary for function. For example, localized disorder in the membrane surface correlates with the activity of phospholipase A_2 whose lipolytic action requires protein insertion from the aqueous phase in the bilayer (58, 59). Furthermore, inverse correlation between the function of HDL particles and their stability suggests that moderate destabilization enhances HDL function, probably by increasing local structural disorder in the lipoprotein surface, and thereby facilitating the insertion of plasma factors, such as lipases and lipid transfer proteins, during metabolic lipoprotein remodeling (60). Similarly, the insertion of LpL in VLDL surface is necessary for the hydrolysis of core TG, an obligatory rate-limiting step in VLDL catabolism (Figure 1). Since mild oxidation destabilizes VLDL (Figure 3A,B and Supporting Information Figure S2), it is expected to accelerate LpL insertion and the ensuing lipolysis. We propose that this may accelerate VLDL metabolism and help to reduce the levels of circulating VLDL. At the same time, reduction in VLDL stability is expected to facilitate VLDL fusion, rupture and lipid droplet formation in the arterial wall, which is proatherogenic (7, 8).

A unique property of VLDL, which reflects the presence of both exchangeable and nonexchangeable proteins in its surface, is fission of small HDL-size particles. Such fission is observed in response to various perturbations that shift the balance between the VLDL core and surface. Thus, TG hydrolysis by LpL produces excess surface material that fissions in the form of apoE-containing HDL. Similarly, oxidative hydrolysis of core lipids probably contributes to fission of HDL-size particles upon VLDL oxidation. Fission of small apoE-containing particles from VLDL upon LpL reaction, heating (37), and/or oxidation (Figures 6 and 7 and Supporting Information Figure S3) implies that such particles form kinetically stable assemblies that are recurring motifs during VLDL remodeling.

Taken together, our results prompt us to hypothesize that mild oxidation that does not impair the ability of apoC-II to activate LpL may accelerate the major rate-limiting step in VLDL remodeling, which involves LpL insertion into VLDL and the ensuing TG hydrolysis, followed by fission of apoE-containing HDL. Mild oxidation, which also involves TG hydrolysis and fission of apoE-containing HDL-size particles, is expected to be synergistic with this step and, hence, accelerate VLDL remodeling. Hence, VLDL stability must be

delicately balanced to allow rapid metabolic remodeling by LpL, which is antiatherogenic, yet minimize VLDL fusion in the arterial wall, which is proatherogenic.

Supplementary Material

Refer to Web version on PubMed Central for supplementary material.

Acknowledgments

We are grateful to Michael Gigliotti and Cheryl England for help with lipoprotein isolation and biochemical analyses and to Donald L. Gantz for help with electron microscopy. We thank Drs. Haya Herscovitz, Shobini Jayaraman, and Xuan Gao for generous help and useful discussions. We are grateful to Dr. D. M. Small for reading the manuscript prior to publication.

References

1. Adiels M, Olofsson SO, Taskinen MR, Borén J. Overproduction of very low-density lipoproteins is the hallmark of the dyslipidemia in the metabolic syndrome. Arterioscler, Thromb, Vasc Biol. 2008; 28(7):1225–1236. [PubMed: 18565848]
2. Therond P. Catabolism of lipoproteins and metabolic syndrome. Curr Opin Clin Nutr Metab Care. 2009; 12(4):366–371. [PubMed: 19474714]
3. Roberts CK, Sindhu KK. Oxidative stress and metabolic syndrome. Life Sci. 2009; 84(21):705–712. [PubMed: 19281826]
4. Havel RJ. Triglyceride-rich lipoproteins and plasma lipid transport. Arterioscler, Thromb, Vasc Biol. 2010; 30(1):9–19. [PubMed: 20018941]
5. Cannon CP. Mixed dyslipidemia, metabolic syndrome, diabetes mellitus, and cardiovascular disease: clinical implications. Am J Cardiol. 2008; 102(12A):5L–9L.
6. Ginsberg HN, MacCallum PR. The obesity, metabolic syndrome, and type 2 diabetes mellitus pandemic: Part I. Increased cardiovascular disease risk and the importance of atherogenic dyslipidemia in persons with the metabolic syndrome and type 2 diabetes mellitus. J Cardiometab Syndr. 2009; 4(2):113–119. [PubMed: 19614799]
7. Krauss RM. Atherogenicity of triglyceride-rich lipoproteins. Am J Cardiol. 1998; 81(4A):13B–17B.
8. Skalen K, Gustafsson M, Rydberg EK, Hulten LM, Wiklund O, Innerarity TL, Boren J. Subendothelial retention of atherogenic lipoproteins in early atherosclerosis. Nature. 2002; 417:750–754. [PubMed: 12066187]
9. Olofsson SO, Boren J. Apolipoprotein B: a clinically important apolipoprotein which assembles atherogenic lipoproteins and promotes the development of atherosclerosis. J Intern Med. 2005; 258(5):395–410. [PubMed: 16238675]
10. Kannel WB, Vasan RS. Triglycerides as vascular risk factors: new epidemiologic insights. Curr Opin Cardiol. 2009; 24:345–350. [PubMed: 19424059]
11. Dallinga-Thie GM, Franssen R, Mooij HL, Visser ME, Hassing HC, Peelman F, Kastelein JJ, Péterfy M, Nieuwdorp M. The metabolism of triglyceride-rich lipoproteins revisited: new players, new insight. Atherosclerosis. 2010; 211(1):1–8. [PubMed: 20117784]
12. Farmer JA, Gotto AM Jr. Currently available hypolipidaemic drugs and future therapeutic developments. Baillieres Clin Endocrinol Metab. 1995; 9(4):825–847. [PubMed: 8593127]
13. Nesto RW. Beyond low-density lipoprotein: addressing the atherogenic lipid triad in type 2 diabetes mellitus and the metabolic syndrome. Am J Cardiovasc Drugs. 2005; 5(6):379–387. [PubMed: 16259526]
14. Davidson MH. Mechanisms for the hypotriglyceridemic effect of marine omega-3 fatty acids. Am J Cardiol. 2006; 98(4A):27i–33i.
15. Segrest JP, Jones MK, De Loof H, Dashti N. Structure of apolipoprotein B-100 in low density lipoproteins. J Lipid Res. 2001; 42(9):1346–1367. [PubMed: 11518754]

16. Merkel M, Eckel RH, Goldberg IJ. Lipoprotein lipase: genetics, lipid uptake, and regulation. J Lipid Res. 2002; 43(12):1997–2006. [PubMed: 12454259]
17. Otarod JK, Goldberg IJ. Lipoprotein lipase and its role in regulation of plasma lipoproteins and cardiac risk. Curr Atheroscler Rep. 2004; 6(5):335–342. [PubMed: 15296698]
18. Wang H, Eckel RH. Lipoprotein lipase: from gene to obesity. Am J Physiol Endocrinol Metab. 2009; 297(2):E271–E288. [PubMed: 19318514]
19. Kolovou GD, Kostakou PM, Anagnostopoulou KK, Cokkinos DV. Therapeutic effects of fibrates in postprandial lipemia. Am J Cardiovasc Drugs. 2008; 8(4):243–255. [PubMed: 18690758]
20. Breckenridge WC. The catabolism of very low density lipoproteins. Can J Biochem Cell Biol. 1985; 63(8):890–897. [PubMed: 3904951]
21. Musliner TA, Long MD, Forte TM, Nichols AV, Gong EL, Blanche PJ, Krauss RM. Dissociation of high density lipoprotein precursors from apolipoprotein B-containing lipoproteins in the presence of unesterified fatty acids and a source of apolipoprotein A-I. J Lipid Res. 1991; 32(6):917–933. [PubMed: 1940624]
22. Krimbou L, Marcil M, Chiba H, Genest J Jr. Structural and functional properties of human plasma high density-sized lipoprotein containing only apoE particles. J Lipid Res. 2003; 44(5):884–892. [PubMed: 12611904]
23. Williams KJ, Fisher EA. Oxidation, lipoproteins, and atherosclerosis: which is wrong, the antioxidants or the theory? Curr Opin Clin Nutr Metab Care. 2005; 8(2):139–146. [PubMed: 15716791]
24. Steinberg D. Low density lipoprotein oxidation and its pathobiological significance. J Biol Chem. 1997; 272:20963–20966. [PubMed: 9261091]
25. Schaefer EJ. Lipoproteins, nutrition, and heart disease. Am J Clin Nutr. 2002; 75:191–212. [PubMed: 11815309]
26. Mohr D, Stocker R. Radical-mediated oxidation of isolated human very-low-density lipoprotein. Arterioscler Thromb. 1994; 14(7):1186–1192. [PubMed: 8018676]
27. Whitman SC, Sawyez CG, Miller DB, Wolfe BM, Huff MW. Oxidized type IV hypertriglyceridemic VLDL-remnants cause greater macrophage cholesteryl ester accumulation than oxidized LDL. J Lipid Res. 1998; 39(5):1008–1020. [PubMed: 9610767]
28. Whitman SC, Hazen SL, Miller DB, Hegele RA, Heinecke JW, Huff MW. Modification of type III VLDL, their remnants, and VLDL from apoE-knockout mice by p-hydroxyphenylacetaldehyde, a product of myeloperoxidase activity, causes marked cholesteryl ester accumulation in macrophages. Arterioscler, Thromb, Vasc Biol. 1999; 19(5):1238–1249. [PubMed: 10323775]
29. Matsuura E, Hughes GR, Khamashta MA. Oxidation of LDL and its clinical implication. Autoimmun Rev. 2008; 7:558–566. [PubMed: 18625445]
30. Bonomini F, Tengattini S, Fabiano A, Bianchi R, Rezzani R. Atherosclerosis and oxidative stress. Histol Histopathol. 2008; 23:381–390. [PubMed: 18072094]
31. Kaneto H, Katakami N, Kawamori D, Miyatsuka T, Sakamoto K, Matsuoka TA, Matsuhisa M, Yamasaki Y. Involvement of oxidative stress in the pathogenesis of diabetes. Antioxid Redox Signal. 2007; 9:355–366. [PubMed: 17184181]
32. Heinecke JW. Is the emperor wearing clothes? Clinical trials of vitamin E and the LDL oxidation hypothesis. Arterioscler, Thromb, Vasc Biol. 2001; 21(8):1261–1264. [PubMed: 11498450]
33. Parthasarathy S, Raghavamenon A, Garelnabi MO, Santanam N. Oxidized low-density lipoprotein. Methods Mol Biol. 2010; 610:403–417. [PubMed: 20013192]
34. Plaisance EP, Grandjean PW, Mahurin AJ. Independent and combined effects of aerobic exercise and pharmacological strategies on serum triglyceride concentrations: a qualitative review. Phys Sportsmed. 2009; 37(1):11–19.
35. Mehta R, Gantz DL, Gursky O. Human plasma high-density lipoproteins are stabilized by kinetic factors. J Mol Biol. 2003; 328(1):183–192. [PubMed: 12684007]
36. Jayaraman S, Gantz DL, Gursky O. Structural basis for thermal stability of human low-density lipoprotein. Biochemistry. 2005; 44(10):3965–3971. [PubMed: 15751972]
37. Guha M, England CO, Herscovitz H, Gursky O. Thermal transitions in human very low-density lipoprotein: fusion, rupture and dissociation of HDL-like particles. Biochemistry. 2007; 46(20): 6043–6049. [PubMed: 17469851]

38. Chung BH, Tallis G, Yalamoori V, Anantharamaiah GM, Segrest JP. Liposome-like particles isolated from human atherosclerotic plaques are structurally and compositionally similar to surface remnants of triglyceride-rich lipoproteins. Arterioscler Thromb. 1994; 14(4):622–635. [PubMed: 8148360]
39. Arai H, Kashivagi S, Nagasaka Y, Uchida K, Hoshii Y, Nakamura K. Oxidative modification of apolipoprotein E in human very low-density lipoprotein and its inhibition by glycosaminoglycans. Arch Biochem Biophys. 1999; 367:1–8. [PubMed: 10375392]
40. Esterbauer H, Striegl G, Puhl H, Rotheneder M. Continuous monitoring of in vitro oxidation of human low density lipoprotein. Free Radical Res Commun. 1989; 6(1):67–75. [PubMed: 2722022]
41. Burkitt MJ. A critical overview of the chemistry of copper-dependent low density lipoprotein oxidation: roles of lipid hydroperoxides, alpha-tocopherol, thiols, and ceruloplasmin. Arch Biochem Biophys. 2001; 394(1):117–135. [PubMed: 11566034]
42. Malle E, Marsche G, Arnhold J, Davies MJ. Modification of low-density lipoprotein by myeloperoxidase-derived oxidants and reagent hypochlorous acid. Biochim Biophys Acta. 2006; 1761(4):392–415. [PubMed: 16698314]
43. Schumaker VN, Puppione DL. Sequential flotation ultracentrifugation. Methods Enzymol. 1986; 128:155–170. [PubMed: 3724500]
44. Gao X, Jayaraman S, Gursky O. Mild oxidation promotes and advanced oxidation prevents protein dissociation and remodeling of human plasma high-density lipoprotein *in vitro*. J Mol Biol. 2008; 376(4):997–1007. [PubMed: 18190928]
45. Jayaraman S, Gantz DL, Gursky O. Effects of oxidation on the structure and stability of human low-density lipoprotein. Biochemistry. 2007; 46(19):5790–5797. [PubMed: 17444660]
46. Whitman SC, Miller DB, Wolfe BM, Hegele RA, Huff MW. Uptake of type III hypertriglyceridemic VLDL by macrophages is enhanced by oxidation, especially after remnant formation. Arterioscler, Thromb, Vasc Biol. 1997; 17(9):1707–1715. [PubMed: 9327767]
47. Benjwal S, Verma S, Rohm KH, Gursky O. Monitoring protein aggregation during thermal unfolding in circular dichroism experiments. Protein Sci. 2006; 15:635–639. [PubMed: 16452626]
48. Parasassi T, Bittolo-Bon G, Brunelli R, Cazzolato G, Krasnowska EK, Mei G, Sevanian A, Ursini F.) Loss of apoB-100 secondary structure and conformation in hydroperoxide rich, electronegative LDL(−). Free Radical Biol Med. 2001; 31(1):82–89. [PubMed: 11425493]
49. Zhang L, Song J, Newhouse Y, Zhang S, Weisgraber KH, Ren G. An optimized negative-staining protocol of electron microscopy for apoE4 POPC lipoprotein. J Lipid Res. 2010; 51(5):1228–1236. [PubMed: 19965615]
50. Jolivalt C, Leininger-Muller B, Drozdz R, Naskalski JW, Siest G. Apolipoprotein E is highly susceptible to oxidation by myeloperoxidase, an enzyme present in the brain. Neurosci Lett. 1996; 210(1):61–64. [PubMed: 8762192]
51. Jayaraman S, Gantz DL, Gursky O. Effects of protein oxidation on the structure and stability of model discoidal high-density lipoproteins. Biochemistry. 2008; 47(12):3875–3882. [PubMed: 18302337]
52. Anantharamaiah GM, Hughes TA, Iqbal M, Gawish A, Neame PJ, Medley MF, Segrest JP. Effect of oxidation on the properties of apolipoproteins A-I and A-II. J Lipid Res. 1988; 29:309–318. [PubMed: 3132519]
53. Jayaraman S, Gantz DL, Gursky O. Kinetic stabilization and fusion of discoidal lipoproteins containing human apoA-2 and DMPC: Comparison with apoA-1 and C-1. Biophys J. 2005; 88(4): 2907–2918. [PubMed: 15681655]
54. Hakala JK, Öörni K, Pentikäinen MO, Hurt-Camejo E, Kovanen PT. Lipolysis of LDL by human secretory phospholipase A_2 induces particle fusion and enhances the retention of LDL to human aortic proteoglycans. Arterioscler, Thromb, Vasc Biol. 2001; 21:1053–1058. [PubMed: 11397719]
55. Kozlovsky Y, Kozlov MM. Membrane fission: model for intermediate structures. Biophys J. 2003; 85(1):85–96. [PubMed: 12829467]
56. Han H-S, Kim H. Spontaneous fragmentation of dimyristoylphosphatidylcholine vesicles into a discoidal form at low pH. J Biochem. 1994; 115(1):26–31. [PubMed: 8188631]
57. Haque ME, Lentz BR. Roles of curvature and hydrophobic interstice energy in fusion: studies of lipid perturbant effects. Biochemistry. 2004; 43(12):3507–3517. [PubMed: 15035621]

58. Burack WR, Biltonen RL. Lipid bilayer heterogeneities and modulation of phospholipase A2 activity. Chem Phys Lipids. 1994; 73(1–2):209–222. [PubMed: 8001182]

59. Ray S, Scott JL, Tatulian SA. Effects of lipid phase transition and membrane surface charge on the interfacial activation of phospholipase A2. Biochemistry. 2007; 46(45):13089–13100. [PubMed: 17944488]

60. Guha M, Gao X, Jayaraman S, Gursky O. Structural stability and functional remodeling of high-density lipoproteins: The importance of being disordered. Biochemistry. 2008; 47(44):11393–11397. [PubMed: 18839964]

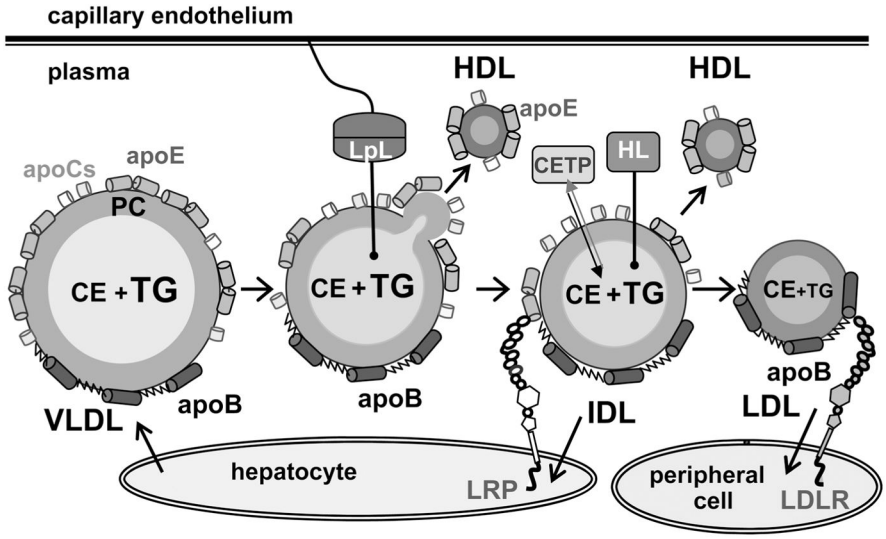

Figure 1.

Remodeling of very low density lipoproteins (VLDL) into intermediate-, low-, and high-density lipoproteins (IDL, LDL, and HDL) in plasma. VLDL, which are secreted by the liver, are remodeled by lipoprotein lipase (LpL) that is tethered to the capillary endothelium via heparin sulfate proteoglycans. LpL hydrolyzes core TG and produces monoacylglycerol and free fatty acids that redistribute from the particle core to its surface. This generates excess surface material that fissions in the form of HDL that contain only exchangeable proteins such as apoE. VLDL remnants (i.e., IDL) are cleared from circulation by receptors such as LDL receptor-related protein (LRP) or scavenger receptors (not shown). Alternatively, IDL are remodeled by hepatic lipase (HL) that hydrolyzes core TG and by cholesterol ester transfer protein (CETP) that exchanges TG for CE. The resulting LDL, which have apoB as their sole protein, are taken up by the LDL receptor (LDLR) or, in their modified forms, by the scavenger receptors in peripheral tissues.

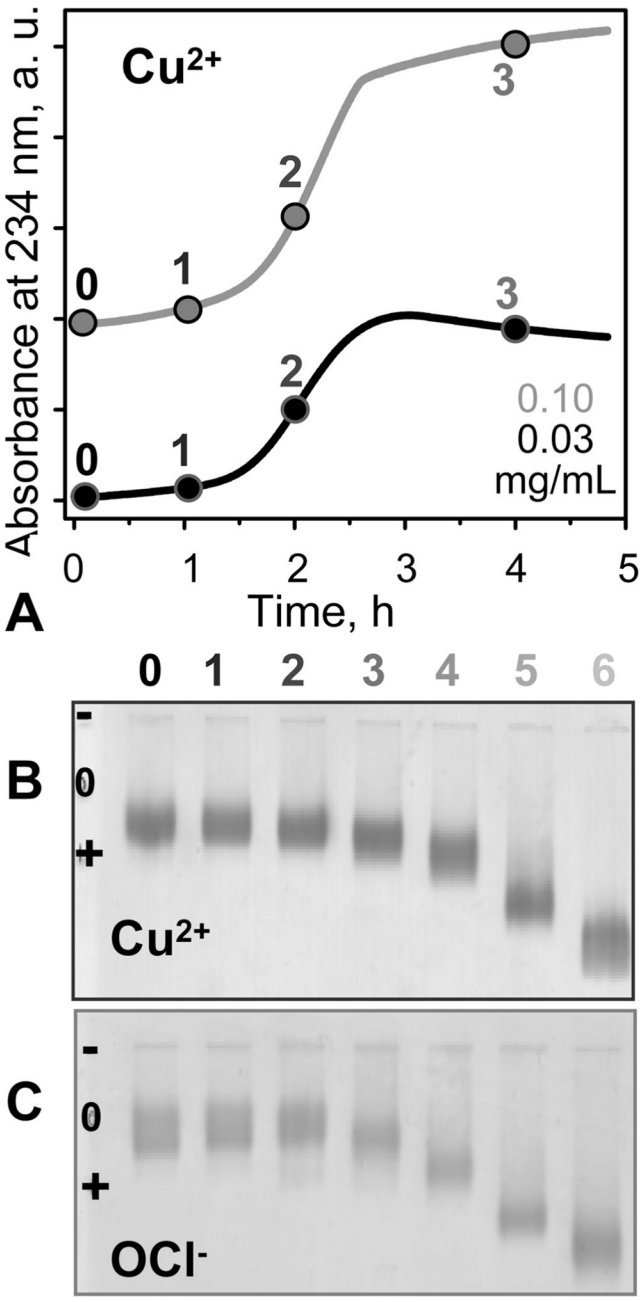

Figure 2.

VLDL oxidation to various stages by Cu^{2+} or OCl^{-}. (A, B) VLDL in EDTA-free standard buffer (5 mM sodium phosphate, 0.02% NaN_3, pH 7.6) were incubated at 37 °C with 5 μM $CuSO_4$ for up to 48 h. (A) The time course of VLDL oxidation by copper was monitored by absorbance at 234 nm for conjugated diene formation. The absorbance is presented for the first 5 h of incubation; no additional changes were observed after further incubation. (B) Agarose gel electrophoresis monitors changes in electronegativity resulting from oxidative Lys modifications and formation of free fatty acids (FFA). Numbers in (A) and (B) correspond to incubation times of 1 h (1), 2 h (2), 4 h (3), 12 h (4), 24 h (5), and 48 h (6); 0

stands for intact VLDL. (C) VLDL in standard buffer (5 mM sodium phosphate, 0.02% NaN_3, 0.25 mM EDTA, pH 7.6) was oxidized to various stages by incubating for 12 h at 37 °C in NaOCl solutions of 0.045 (1), 0.2 (2), 0.5 (3), 0.8 (4), 1.0 (5), and 5.0 mM (6) concentration. VLDL protein concentrations are 0.03 (black) or 0.1 mg/mL (gray) in (A) and 0.5 mg/mL in (B) and (C).

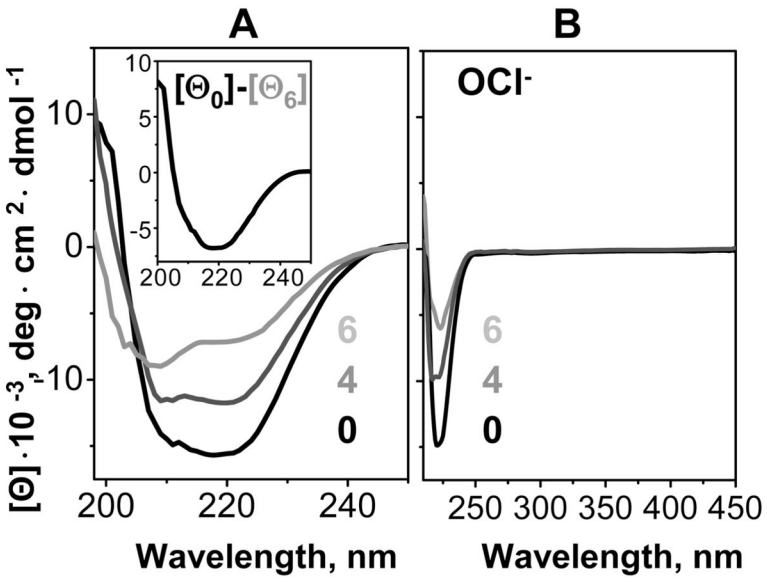

Figure 3.

Circular dichroism spectra of intact and oxidized VLDL. $VLDL_2$ were oxidized by OCl^- to stages 1–6 as described in Figure 2 legend and in Materials and Methods; 0 stands for intact VLDL. The samples were diluted to 0.1 mg/mL protein to record far-UV CD (A) or used at 0.5 mg/mL protein to record far- and near-UV CD (B). Insert: Difference spectrum between the far-UV CD of $VLDL_2$ that were intact or oxidized to stage 6, $[\Theta_0]$–$[\Theta_6]$; negative peak centered at 218 nm, which is characteristic of the β-sheet, indicates β-sheet unfolding upon oxidation. Near-UV CD above 300 nm remained invariant (B), suggesting that VLDL did not rupture upon oxidation (37).

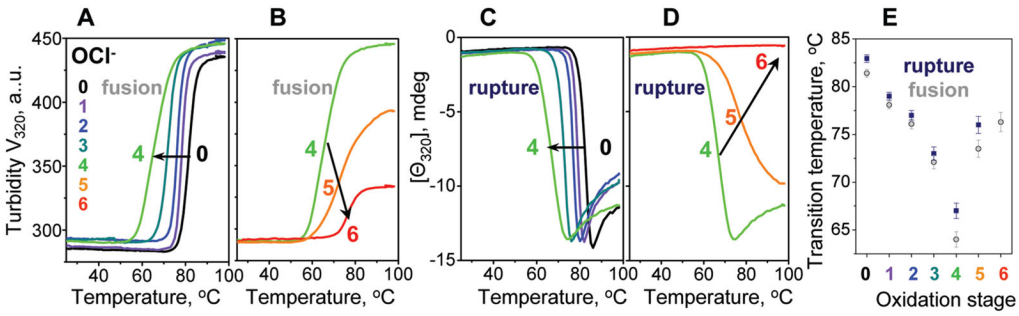

Figure 4.

Effects of oxidation on the apparent thermal stability of VLDL. $VLDL_2$ that were intact (0) or oxidized by OCl^- to stages 1–6 were diluted to 0.1 mg/mL protein in standard buffer and heated at a rate of 11 °C/h. Increase in the particle size due to VLDL fusion followed by rupture and coalescence into lipid droplets was monitored by turbidity at 320 nm (A, B), which is proportional to the dynode voltage V_{320} measured in CD experiments (47). Repacking of apolar core lipids upon VLDL rupture and coalescence into lipid droplets was monitored by CD at 320 nm, $\Theta_{320}(T)$ (C, D), that was measured simultaneously with $V_{320}(T)$ (A, B). Arrows indicate changes in the heating data upon progressive oxidation. (E) The apparent transition temperatures, which were determined from the peak positions in the first derivatives of the melting data, $dV_{320}(T)/dT$ (for fusion and rupture) and $d\Theta_{320}(T)/dT$ (for rupture), are plotted as a function of oxidation stage. Error bars reflect accuracy in T_m determination.

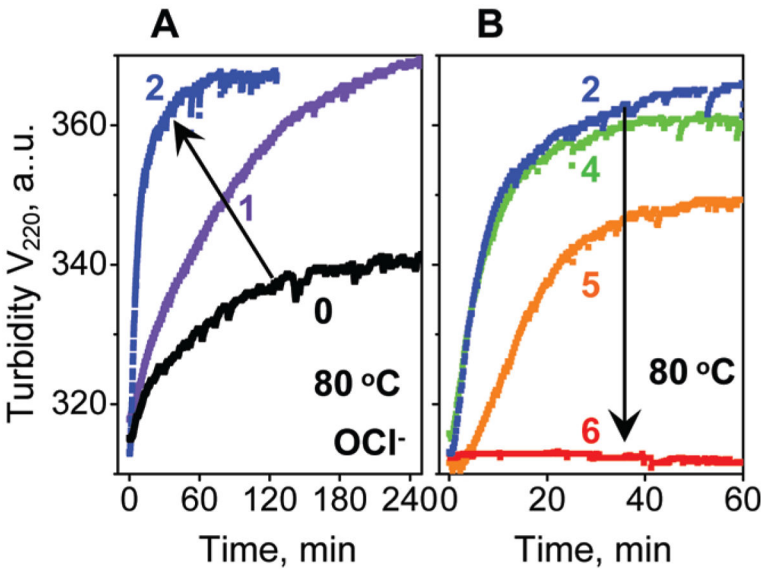

Figure 5.

Effects of oxidation on thermal denaturation kinetics of VLDL. $VLDL_2$ that were intact (0) or oxidized by OCl^- to stages 1–6 were diluted to 0.1 mg/mL protein in a standard buffer and subjected to temperature jumps from 25 to 80 °C. Time course of changes in the particle size due to VLDL fusion followed by rupture and coalescence into lipid droplets was monitored by turbidity at 220 nm, $V_{220}(t)$. Arrows indicate changes in the transition kinetics upon VLDL oxidation.

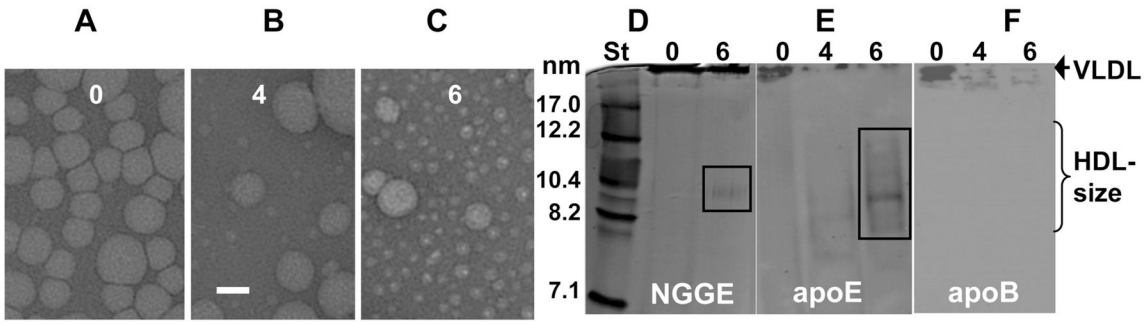

Figure 6.

Effects of VLDL oxidation on the particle morphology at ambient temperatures. Total plasma VLDL that were intact (0) or oxidized by Cu^{2+} to stages 4 or 6 were visualized by negative stain electron microscopy at 22 °C (A, B, C) and were subjected to nondenaturing gradient gel electrophoresis (NGGE) using 4–20% gradient (D) followed by immunoblotting for apoE (E) or apoB (F). The gels were stained with Imperial protein stain. Numbers indicate oxidation stages. Bar size in panel B is 40 nm.

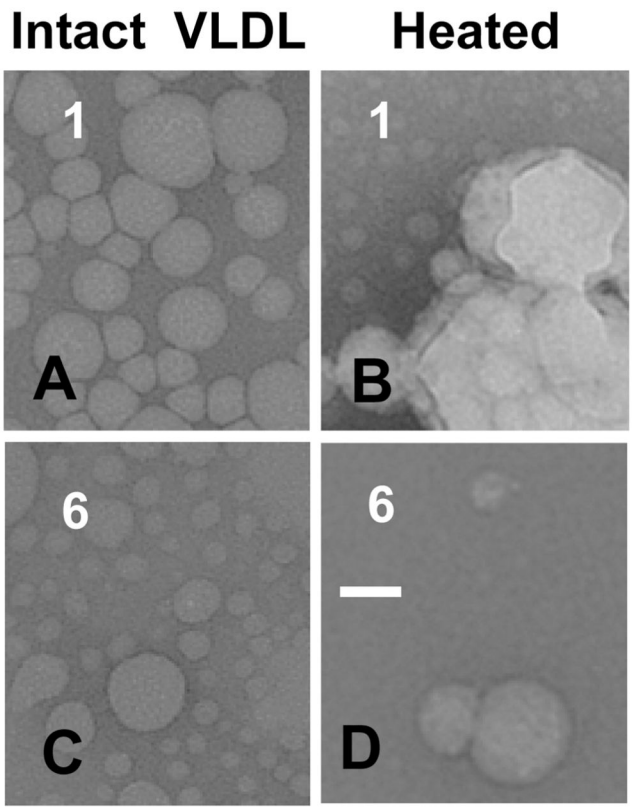

Figure 7.

Effects of oxidation on the heat-induced changes in the particle morphology. VLDL that were oxidized by Cu^{2+} to stage 1 or 6 (indicated) were heated to 99 °C, cooled to 25 °C, and visualized by negative staining EM. Bar size is 40 nm.

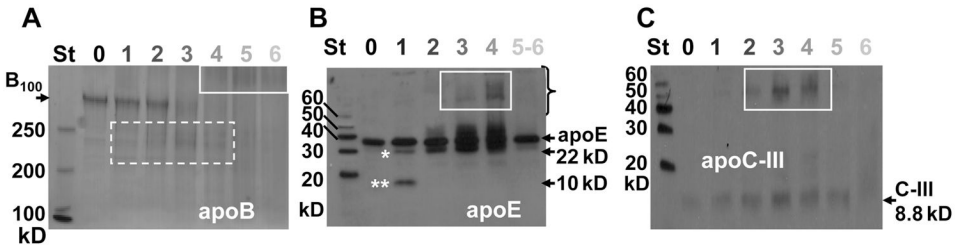

Figure 8.

Oxidative changes in VLDL proteins assessed by SDS–PAGE. VLDL that were intact (0) or oxidized by OCl^- to stages 1–6 (shown on the lane numbers) were analyzed. (A) 4% SDS–PAGE stained with Imperial protein stain; arrow indicates full-size apoB (B_{100}, 550 kDa); dashed box illustrates apoB fragments. (B) 12% SDS–PAGE followed by immunoblotting for apoE; arrows indicate intact apoE (32 kDa) and its N-terminal 22 kDa (*) and C-terminal 10 kDa (**) fragments. (C) 20% SDS–PAGE followed by immunoblotting for apoC-III; arrow indicates apoC-III (8.8 kDa). Solid white boxes in all panels indicate cross-linked proteins.

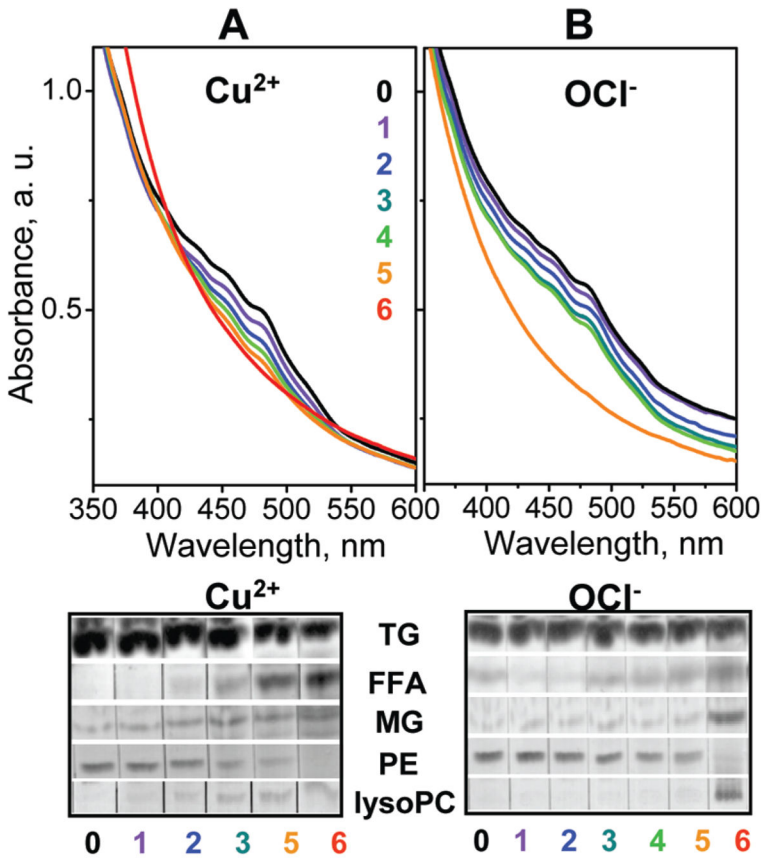

Figure 9.

Oxidative changes in VLDL lipids monitored by absorption spectroscopy and thin-layer chromatography. VLDL were intact (0) or oxidized by Cu^{2+} (A) or OCl^{-} (B) to stages 1–6 (indicated). Top panels:Visible absorption spectra show changes in the levels of carotenoids in VLDL core upon oxidation. Bottom panels: TLC shows changes in the levels of VLDL lipids, including TG, FFA, MG, PE, and lyso-PC, upon oxidation.